RUNNING TITLE: Mercury, dissolved organic matter, and microbiomes

Trends in dissolved organic matter cycling, sediment microbiomes, and methylmercury production across vegetation heterogeneity in a Great Lakes wetland

Emily B. Graham[1*], Joseph E. Knelman[2], Rachel S. Gabor[3], Shon Schooler[4], Diane M. McKnight[2,5,6], Diana R. Nemergut[2,7]

[1]Biological Sciences Division, Pacific Northwest National Laboratory, Richland, WA, USA

[2] Institute for Arctic and Alpine Research, University of Colorado at Boulder, Boulder, CO, USA

[3]School of Environment and Natural Resources, The Ohio State University, Columbus, OH, USA

[4]Lake Superior National Estuarine Research Reserve, University of Wisconsin-Superior, Superior, WI, USA

[5]Civil Engineering Department, University of Colorado at Boulder, Boulder, CO, USA

[6]Environmental Studies Program, University of Colorado at Boulder, Boulder, CO, USA

[7]Biology Department, Duke University, Durham, NC, USA

The authors declare no conflict of interest.

Correspondence: Emily B. Graham, emily.graham@colorado.edu; Biological Sciences Division; Pacific Northwest National Laboratory; 902 Battelle Blvd.; Richland, WA, 99354; (509) 372-6049

Abstract.

Recent advances have allowed for greater investigation into microbial regulation of mercury toxicity in the environment. In wetlands in particular, dissolved organic matter (DOM) may influence methylmercury (MeHg) production both through chemical interactions and through substrate effects on microbiomes. We conducted microcosm experiments in two disparate wetland environments (oligotrophic unvegetated and high-C vegetated sediments) to examine the impacts of plant leachate and inorganic mercury loadings (20 mg/L $HgCl_2$) on microbiomes, DOM cycling, and MeHg production in the St. Louis River Estuary. Our research reveals the greater relative capacity for mercury methylation in vegetated over unvegetated sediments. Further, our work shows how mercury cycling in oligotrophic unvegetated sediments may be susceptible to DOM inputs in the St. Louis River Estuary: microcosms receiving leachate produced substantially more MeHg than unamended microcosms. We also demonstrate (1) changes in microbiome structure towards *Clostridia*, (2) metagenomic shifts toward fermentation, and (3) degradation of complex DOM; all of which coincide with elevated net MeHg production in unvegetated microcosms receiving leachate. Finally, we examine microbial operational taxonomic units (OTUs) classified as known potential methylators and identify important organisms for future research in the Great Lakes region. Together, our work shows the influence of wetland vegetation in controlling MeHg production in the Great Lakes region and provides evidence that this may be due to both enhanced microbial activity as well as differences in microbiome composition.

Keywords. St. Louis River Estuary, Clostridia, oligotrophic, fermentation, mercury methylation, carbon

Introduction.

Mercury methylation in anoxic sediments is central to the bioaccumulation of mercury in plant and animal tissue (Benoit et al., 2003; Morel et al., 1998; Ullrich et al., 2001) and poses a significant environmental and human health concern in the freshwater wetlands of the Great Lakes region (Branfireun et al., 1999; Harmon et al., 2005; Jeremiason et al., 2006). Dissolved organic matter (DOM) has been a focus of geochemical investigations for decades, and both positive and negative interactions between DOM and mercury methylation – principally, a microbial transformation (Hsu-Kim et al., 2013) – have been demonstrated under contrasting environmental conditions (Graham et al., 2013; Hsu-Kim et al., 2013; Ravichandran, 2004). Yet, linkages among DOM cycling, sediment microbiomes that directly mediate mercury methylation, and MeHg production remain poorly described.

Dissolved organic matter is comprised of various classes of organic compounds (primarily organic acids) with a wide range of molecular weights and aromaticities (Lambertsson and Nilsson, 2006; Wetzel, 1992). DOM concentrations are elevated in wetlands relative to other freshwater systems (>10 mg/L), and the humic fraction derived from plant leachate predominates. With respect to mercury cycling in wetlands, mercury methylation is impacted both by binding properties of the humic DOM fraction, resulting either in increased dissolution of inorganic mercury complexes or in physical inhibition of mercury bioavailability (Drexel et al., 2002; Haitzer et al., 2002; Waples et al., 2005), and by the provisioning of organic substrate for microbial activity (Hsu-Kim et al., 2013; King et al., 2000; Lambertsson and Nilsson, 2006). These effects may also vary with ambient geochemistry. For instance, Graham *et al.* (2013) have demonstrated that sulfide concentrations and DOM aromaticity interact to influence MeHg production. Further, interactive effects of sediment microbiomes and DOM biogeochemistry are

less-well resolved than other aspects of linkages between environmental geochemistry and mercury toxicity. Since mercury methylation is strongly impacted by DOM, environments such as the St. Louis River estuary, which contains areas of both vegetated and unvegetated sediments, may also show differences in the capacity for MeHg production across vegetation gradients which exhibit pronounced differences in DOM content. Numerous studies have shown that microbiome composition is influenced by DOM quantity and/or quality (Docherty et al., 2006; Forsström et al., 2013; Graham et al., 2016a, 2017; Pernthaler, 2013; Stegen et al., 2016), and such changes in environmental microbiomes alter biogeochemistry (Graham et al., 2016a, 2017; Graham et al., 2016b). The character of humic DOM (putatively most influential to mercury methylation) can be assessed at scales relevant to microbial activity with fluorescence spectroscopy, which can be easily applied in natural settings (Fellman et al., 2010).

While the microbial mechanisms generating methylmercury are poorly understood, the recent discovery of the *hgcAB* gene cluster has allowed investigations into the microbial ecology of mercury cycling (Boyd et al., 2017; Gilmour et al., 2013; Gionfriddo et al., 2016; Parks et al., 2013; Rani et al., 2015; Rothenberg et al., 2016; Schwartz et al., 2016). In particular, interactions between environmental microbiomes, DOM quantity and quality, and mercury methylation in natural systems remain an uncertainty in predicting hotspots of mercury toxicity in the environment (Hsu-Kim et al., 2013; Podar et al., 2015). Recent work has increased knowledge on the microbiology of mercury methylation, expanding potential microorganisms mediating methylation beyond sulfate-reducing bacteria (Compeau and Bartha, 1985; Hsu-Kim et al., 2013), iron-reducing bacteria (Kerin et al., 2006) and methanogens (Hamelin et al., 2011). For example, Gionfriddo et al. (2016) and Rani et al. (2015) have leveraged new molecular

techniques to discover relationships between newly identified organisms and MeHg production in sea ice and dental wastewater, respectively.

These new organisms are an emerging research frontier; and resolving interactions between sediment microbiomes, environmental chemistry, and inorganic mercury complexes remains central in understanding variation in methylation rates among natural systems (Gilmour et al., 2013; Hintelmann et al., 2000; Hsu-Kim et al., 2013). All microorganisms containing the *hgcAB* gene cluster that been tested to date are confirmed methylators, and the gene appears to be highly conserved allowing it to serve as a genetic marker for methylating organisms (Christensen et al., 2016; Gilmour et al., 2013; Hsu-Kim et al., 2013). Gilmour *et al.* (2013) have identified five clades of putative methylators, including new clades of syntrophic and *Clostridial* organisms. Some research has provided insight into the abundance of these new organisms in mercury-contaminated landscapes (Bae et al., 2014; Gionfriddo et al., 2016; Hamelin et al., 2015; Liu et al., 2014a; Rani et al., 2015; Rothenberg et al., 2016), but many studies have continued to focus on the involvement of sulfate- (Boyd et al., 2017; Liu et al., 2014b; Lu et al., 2016; Schwartz et al., 2016) and iron-reducing bacteria (Si et al., 2015) as well as methanogens (Yu et al., 2013) in mercury methylation.

In this study, we examine the influence of DOM from plant leachate on net methylmercury (MeHg) production in a contaminated freshwater estuary at the base of Lake Superior. First, we describe net MeHg production in environments associated with ambient DOM concentration that are high (vegetated sediments) and low (unvegetated sediments). We hypothesize that both DOM quantity and quality influence mercury methylation through two different pathways, 1) by regulating microbial activity and 2) by shifting the metabolic diversity of mercury methylators. We test this hypothesis across chemically distinct sediments associated

with unvegetated (oligotrophic, low-C) and vegetated (high-C) environments. We used a microcosm experiment to monitor changes in sediment microbiomes, DOM chemical quality, and net MeHg production in response to additions of leachate from overlying plant material. DOM quality was characterized by fluorescence spectroscopy using indices that can be incorporated in site assessment and monitoring strategies. In total, this work delineates a broad view of how vegetated vs. unvegetated sediments in the St. Louis River Estuary may have different capacities for the cycling of mercury.

Methods.

Field site.

The St. Louis River Estuary is home to the largest U.S. port on the Great Lakes and covers roughly 12,000 acres of wetland habitat directly emptying into Lake Superior. Mining in the headwaters, industrial discharge in the port, and atmospheric deposition have left a legacy of mercury contamination in the sediment. We obtained sediment samples from vegetated (*Zizania palustris* (wild rice), 46° 40.855’ N, 91° 59.048’W) and unvegetated (46° 41.918’ N, 92° 0.123’ W) patches in Allouez Bay and fresh wild rice plant matter from nearby Pokegama Bay (46.683448^{o}N, 92.159261^{o}W) to minimize sampling impacts. Both habitats are clay-influenced embayments that drain an alluvial clay plain created by deposition during the retreat of the last glaciation approximately 10,000 years BP.

Experimental design.

A total of 20 anoxic microcosms were constructed in September 2013 to investigate relationships between DOM cycling, sediment microbiomes, and mercury methylation. Sediment

was obtained in 250-mL amber Nalgene bottles from the top 10 cm of sediment using a block sampling design described in the Supplemental Material. Leachate was extracted using 1 g dried, ground plant matter:20 mL of Nanopure water, filtered through Whatman 0.7 μm GFF filters (Whatman Incorporated, Florham Park, NJ, USA). Microcosms were constructed in 500-mL airtight glass mason jars and stored at room temperature in the dark in Mylar bags with oxygen-absorbing packets between subsampling. Our experiment was designed to promote microbial MeHg production by minimizing abiotic photo-methylation and -demethylation (Morel et al., 1998) and sustaining a low redox environment to inhibit demethylation (Compeau and Bartha, 1984). We acknowledge that we did not eliminate all potential demethylation activity from our microcosms, and we refer to changes in MeHg as 'net MeHg production' to reflect possible demethylation (consistent with other recent work, Schwartz et al., 2016). All experimental set up and sample processing was conducted in an anaerobic glovebox containing 85% N_2, 5% CO_2, and 10% H_2 gas mix at the USGS in Boulder, CO. Jars were degassed in the glovebox for 48 hr prior to experimentation to remove oxygen.

A full-factorial design was employed with two environments (vegetated and unvegetated sediment) and two treatments (plant leachate and Nanopure water). Sediments were homogenized via mixing but unsieved to maintain environment characteristics. Large roots (>1 cm) were infrequent and removed to lessen heterogeneity among replicates. Each microcosm received 100 g wet sediment, and 250 mL solution consisting either of leachate at 100 mg/L (~5x natural concentrations to mimic a loading event) and $HgCl_2$ at 20 mg/L (50 μg/g wet sediment) in Nanopure water (leachate replicates) or solely of $HgCl_2$ at 20 mg/L in nanopure water (no leachate replicates). The purpose of $HgCl_2$ addition at high concentration was to negate initial differences in mercury, overcome $HgCl_2$ inaccessibility due to abiotic organo-metal interactions,

and provide substrate for the duration of the experiment. $HgCl_2$ concentrations were elevated to extreme levels (1,000x ambient concentration), reflecting a convention in ecological change literature to stress ecosystems and eliminate substrate limitation with high levels of nutrients to assist in deciphering mechanistic controls over a process of interest. Although we added more $HgCl_2$ than is common in mercury-DOM literature, we note that (1) the duration of experiment was long relative to other studies (28 days vs. <24hr in many studies); (2) DOM concentrations are high in the St. Louis River Estuary (>20 mg/L in the water column), and (3) added $HgCl_2$ concentrations were of comparable magnitude to some microcosm experiments of similar design (Harris-Hellal et al., 2009; Ruggiero et al., 2011; Zhou et al., 2012). Though we did not directly assess microbial activity, we estimate minimal dosage effects as communities without leachate did not change through time in unvegetated microcosms and only slightly changed through time in vegetated microcosms (R^2 = 0.19, see results and Figure S1). Microcosms were incubated for 28 days, and subsamples of sediment and water were taken every seven days for analysis of sediment microbiomes and DOM characteristics.

Sediment chemistry, extracellular enzyme activity, and mercury methylation.

Percent carbon and nitrogen, NO_3^-/NO_2^-, NH_4^+, total particulate organic carbon (TPOC), total dissolved nitrogen (TDN), pH, and extracellular enzyme activities of β-1,4-glucosidase, β -1,4-N-acetylglucosaminidase, and acid phosphatase were determined on pre-incubation sediments, as described in the Supplemental Material. For total- and methylmercury analysis, initial (day 0) and final (day 28) subsamples were frozen at -70°C, freeze-dried, and sent on dry ice to the USGS Mercury Lab in Middleton, WI for analysis by aqueous phase ethylation, followed by gas chromatographic separation with cold vapor atomic fluorescence detection

(Method 5A-8), acid digestion (Method 5A-7), and QA/QC. Mercury analyses were performed on 3 of 5 replicates for each environment and microcosm type. All other analyses were performed on 5 replicates, except for no unvegetated microcosms without leachate beyond day 0 (n = 4, one replicate destroyed during experiment).

Dissolved organic matter characteristics.

Aqueous subsamples from water overlying sediments were collected at 7-day intervals (days 0, 7, 14, 21, and 28) to determine non-purgeable organic carbon (NPOC) concentration and specific UV absorbance at 254 nm ($SUVA_{254}$) as well characteristics of the optically active DOM pool (mostly associated with humic DOM fraction), as described in the Supplemental Material. We calculated the fluorescence index (FI) to determine the relative contribution of microbial vs. terrestrial matter to the DOM pool, the humic index (HIX) to identify large aromatic compounds consistent with humic material, and the freshness index to determine the availability of labile carbon (Fellman et al., 2010; Gabor et al., 2014a) using MATLAB software (2013a, The MathWorks, Natick, MA) according to Gabor *et al.* (2014b).

Microbial DNA extraction, 16S rRNA amplicon, and metagenomic shotgun sequencing.

DNA from each sediment subsample was extracted using the MO Bio Power Soil DNA Extraction kit (MO BIO Laboratories, Carlsbad, CA, USA), as described in Knelman *et al.*(2012). The region encoding the V4 fragment of the 16S rRNA gene was amplified with the primers 515F/806R, using the PCR protocol described by the Earth Microbiome Project (Caporaso et al., 2012) (Supplemental Material). The final multiplexed DNA samples were sequenced at CU-Boulder (BioFrontiers Institute, Boulder, CO) on an Illumina MiSeq with the

MiSeq Reagent Kit v2, 300 cycles (Illumina, Cat. # MS-102-2002) to generate 2 x 150-bp paired-end reads. Sequences are available at XXXXXX. In addition, 3 unvegetated leachate replicates at day 0 (before leachate addition) and day 28 were sent to the Joint Genome Institute (JGI) for shotgun metagenomic sequencing on the Illumina HiSeq platform. Sequences are available at XXXXX.

Sequence analysis.

Partial 16S rRNA gene were filtered for sequence length and minimum quality score in the UPARSE pipeline (Edgar, 2013) and OTUs were assigned using QIIME (Caporaso et al., 2010) (Supplemental Material). Metagenomic shotgun sequences were assembled and classified against the protein families database (Pfam) (Finn, 2012), Clusters of Orthologous Groups of proteins (COG)(Tatusov et al., 2003), and Kyoto Encyclopedia of Genes and Genomes (KEGG)(Kanehisa and Goto, 2000) by JGI via the IMG database pipeline (Markowitz et al., 2012).

To examine methylator community structure at finer resolution than possible within the full 16S rRNA sequence set, we located 90 of 142 (65%) microbial strains that have been identified as containing the hgcAB gene cluster (listed by Oak Ridge National Laboratory (ORNL), http://www.esd.ornl.gov/programs/rsfa/data/PredictedMethylators/PredictedMethylators_20160420.pdf) with available complete or partial 16S rRNA gene sequences in the NCBI GenBank database (Benson et al., 2013). The represented sequences spanned all clades of methylators (Figure S2). We created a closed-reference database of these sequences and picked OTUs against this database in QIIME. In addition, a BLAST database was constructed from all *hgcA* and *hgcB* gene sequences available in GenBank. A BLASTX search was conducted against this database to

identify taxonomic affiliation of methylators in our samples; however, our query resulted in no matches, likely due to inadequate sequencing depth.

Statistical analysis.

All analyses, unless otherwise noted, were conducted using the *R* software platform. Shapiro-Wilk tests were used to verify normality and assess the appropriateness of parametric vs. non-parametric tests. Multivariate sediment properties (*e.g.*, sediment geochemistry, extracellular enzyme activity, and DNA quantity) were compared across environments at day 0 with Hotelling's T-square Test and post hoc Student's *t*-tests. MeHg production was calculated by subtracting day 0 from day 28 MeHg concentrations; values below detection limit were assigned the detection limit as a value for a conservative estimate of change. MeHg production was compared across groups using ANOVA. Changes in DOM indices (FI, freshness, HIX) through time (days 0, 7, 14, 21, and 28) in each sample group were assessed with linear and quadratic regressions. DOM samples with $SUVA_{254}$ >7 were removed due to fluorescence interference from inorganic molecules. Comparisons of DOM indices between data subsets were conducted with ANOVA and post hoc Tukey HSD.

Microbial community dissimilarity matrices based on 16S rRNA sequences were constructed using the weighted UniFrac method (Lozupone et al., 2011) in QIIME. Alpha diversity for each sample was assessed using the PD whole tree metric in QIIME. Changes in community structure through time (days 0, 7, 14, 21, 28) were assessed with ANOSIM in QIIME. Differences in alpha diversity at day 0 were assessed using unpaired one-way Student's *t*-tests. Relative abundances of major clades were assessed between vegetated and unvegetated environments at day 0 and changes in clades through time (days 0, 7, 14, 21, 28) were assessed

using non-parametric Kruskal-Wallis tests with FDR-correct *P* values. SIMPER analysis was conducted using the 'vegan package' to identify OTUs associated with community dissimilarity between days 0 and 28 in microcosms receiving leachate.

To provide greater resolution into microbiome changes associated with mercury methylation, we used one-sided Mann-Whitney U tests to identify clades of organisms on ORNL's list of potential methylators that changed through time. We build upon previous work by Rothenberg et al. (2016), who examined genus-level changes in known methylating clades, and Rani et al. (2015), who examined only methylating Deltaproteobacteria at the OTU level, by targeting all microorganisms identified by ORNL at the OTU level. We present results as changes in percent relative abundance rather than fold-change due to the absence of some organisms at day 0 (i.e., zero abundance). Microorganisms that exhibited significant changes were further compared to HIX and net MeHg production to parse relationships among all three data types. For this analysis, we used the Pearson product-momentum correlation coefficient, grouping leachate and no leachate microcosms within each environment in a single analysis to provide replication across a wide range of variation (analysis conducted on data from day 28, $n = 6$).

Finally, we explored metagenomic shotgun sequences for information on specific microbial metabolic pathways that changed through time in our microcosms. We used binomial tests to detect increases in the frequency of COGs, Pfams, and KEGG pathways at day 28 relative to day 0. Targets more abundant at day 28 (FDR-corrected $P < 0.01$) were examined for correlations with HIX and MeHg production with the Pearson product-momentum correlation coefficient to decipher possible links between microbial metabolism, DOM cycling, and net MeHg production.

Results.

Ambient geochemistry and microbiology.

Physicochemical properties and sediment microbiomes differed between vegetated and unvegetated environments (Hotelling P = 0.004, Table 1). The unvegetated environment was extremely oligotrophic, with low concentrations of sediment C and N, and both vegetated and unvegetated environments appeared to be N-limited (C:N 16.43 and 20.06). DNA concentration, enzyme activities, and mercury concentrations were an order of magnitude higher within the vegetated environment (Table 1). In addition, methylmercury production in sediments without leachate addition was significantly higher in vegetated sediment than unvegetated sediment, by nearly two orders of magnitude (Figure 1). Final total Hg concentrations at the end of the microcosm experiment were 79.2 +/- 18.3 (vegetated with leachate), 86.5 +/- 14.5 (vegetated without leachate), 15.0 +/- 5.8 (unvegetated with leachate), and 18.1 +/-1.3 ug per g wet sediment. Microbial community structure and alpha diversity were significantly different between the two environments (ANOSIM, P = 0.001, R= 1.00, *t*-test, P = 0.01), though major phyla were similar (Table 1) and both environments were bacteria (vs. archaea) dominated.

Microbiome response to $HgCl_2$ and leachate addition.

Over the course of the incubation, microcosms with vegetated, high-C sediment produced over ten times more MeHg than unvegetated sediment microcosms, regardless of leachate amendment (ANOVA P = 0.002, Figure 1). Mercury methylation was enhanced by leachate within the oligotrophic unvegetated environment with roughly two to four times more production

in microcosms receiving leachate as compared to those without leachate. However, leachate did not stimulate MeHg production in the vegetated environment.

Community structure changed through time in vegetated and unvegetated environments with leachate (ANOSIM across days 0, 7, 14, 21, 28, veg.: P = 0.001 R = 0.40, unveg.: P = 0.001 R = 0.43, Figure S2A and B), but not those without leachate (veg.: P = 0.02, R = 0.19, unveg.: P > 0.05, Figure S2A and B), indicating no substantial effect from high concentrations of added mercury. At day 28, communities in unvegetated microcosms with leachate were different than those without leachate (ANOSIM, P = 0.01, R = 0.54), while microbiome structure in vegetated sediment microcosms only weakly differed between leachate and no leachate groups (P = 0.04, R = 0.22).

Changes in community structure in response to leachate was partially generated by an increase in *Clostridia* in both environments (Kruskal-Wallis, veg.: FDR-corrected P = 0.003, unveg.: P = 0.018, Figure 2B, Table S3) and a decrease in *Deltaproteobacteria* in unvegetated sediment (Kruskal-Wallis, veg.: FDR-corrected P = 0.36, unveg.: FDR-corrected P = 0.015, Figure 2A). In particular, *Clostridia* abundances increased by 3-fold (1.1% to 3.8% of the microbiome) and 10-fold (1.5% to 10.5% of the microbiome), respectively in vegetated and unvegetated environments, driven by increases in nearly all families of *Clostridia*. SIMPER analysis was confirmative of these changes in the full community -- 22.9% of 175 SIMPER-identified OTUs belonged to *Clostridia* (increased from avg. 0.78 OTUs/sample to avg. 17.20 OTUs/sample, Table S3) while 8% belonged to *Deltaproteobacteria* (decreased from avg. 8.5 OTUs/sample to 7.4 OTUs/sample, Table S2).

Changes in the methylating community were more evident at finer taxonomic levels. One family of *Clostridia* (*Peptococcaceae*), sharply increased with leachate in unvegetated sediment

and displayed a similar trend in vegetated sediment (Mann-Whitney U, veg.: uncorrected P = 0.03, unveg.: uncorrected P = 0.03, Figure 2B, Table S3). These changes were due in part to increases in two closely related methylating OTUs (Mann-Whitney U, *Dehalobacter restrictus strain PER-K23,* veg.: uncorrected P = 0.04, from an average of 0% to 6% of methylators, and *Syntrophobotulus glycolicus strain DSM 1351*, unveg.: uncorrected P = 0.01, from an average of 0% to 3% of methylators) grouped in a single genus by our classification system (*Dehalobacter_Syntrophobotulus*, Figure S2). Vegetated sediments also experienced a slight increase in *[Clostridium] cellobioparum strain DSM 1351* (uncorrected P = 0.03, from an average of 0% to 1% of methylators), while unvegetated sediments displayed an increase in *Geobacter bemidjiensis strain Bem* (uncorrected P = 0.02, from an average of 24% to 42% of methylators) and a decrease in *Geobacter sp. M21* (uncorrected P = 0.006, from an average of 15% to 3% of methylators). No other OTUs changes in these microcosms

Metagenomic shotgun sequences were consistent with microbiome shifts observed in 16S rRNA genes. We note increases in *Clostridia* (*t*-test, FDR-corrected P = 0.006), *Peptococcaceae* (*t*-test, FDR-corrected P = 0.018), *Dehalobacter restrictus* (*t*-test, FDR-corrected P = 0.024), and *Syntrophobotulus glycolicus* (*t*-test, FDR-corrected P = 0.042) as well as a possible trend for decreases in *Deltaproteobacteria* (*t*-test, FDR-corrected P = 0.18) in metagenomic data (Figure 3D). We also idenitfied 7,150 KEGG pathways, 84 COGs, and 79 Pfams that were significantly enriched at day 28 relative to day 0 in unvegetated leachate microcosms (Figure 3A-C). All classfication systems revealed metabolic shifts towards glycosyltranseferases, among other pathways involved in DOM oxidation and in iron and nitrate reduction.

Changes in DOM chemistry.

Details of DOM quantity and quality changes are presented in Figures 4 and S3 and described in greater detail in the Supplemental Material. Regression statistics associated with Figures 4 and S3 are presented in Table 2.

DOM fluorescence indices displayed notable changes through time. In the vegetated environment, FI remained stable at a low value in leachate microcosms, indicating plant-derived DOM, and rose in microcosms without leachate indicating greater relative contribution of microbial vs. abiotic processing (Figure 4A and B). In contrast, in the vegetated environment, HIX increased in both leachate and no leachate microcosms indicating processing of more labile vs. recalcitrant DOM (Figure 4C and D). This increase in HIX corresponded with decrease in freshness (Figure 4E and F), further supporting our interpretation. In the unvegetated environment, leachate microcosms (but not microcosms without leachate) increased in FI (Figure 4A and B) denoting an increase in microbially-sourced DOM over time. There was no change in HIX (Figure 4C and D) suggesting equal processing of labile vs. recalcitrant DOM. Freshness varied non-linearly in leachate microcosms but not those without leachate (Figure 4E and F).

Across environment types, HIX was significantly higher in vegetated microcosms (ANOVA $P < 0.0001$, Tukey HSD, leachate: $P < 0.0001$, no leachate: $P = 0.004$). FI and freshness were higher in unvegetated leachate microcosms than in vegetated DOM-amended microcosms (Tukey HSD, FI: $P = 0.003$, freshness: $P = 0.03$) but did not differ across microcosms without leachate (Tukey HSD, FI: $P = 0.89$, freshness: $P = 0.40$).

Correlation of microbiome, DOM characteristics, and MeHg production.

Given the apparent shift in community structure towards *Clostridia*, and (chemoorganotrophic) *Peptococcaceae* in particular, we examined correlations of this family

with the proportion of complex organic matter (HIX) and MeHg production within each environment. We focused on HIX because this index changed consistently and reflected portions of recalcitrant carbon substrate pools utilized by the organisms we identified. Because we only calculated net MeHg production at the conclusion of the incubation, we analyzed these correlations at day 28 and grouped leachate and no-leachate replicates within each environment to provide sufficient variation and sample size (n = 6). *Peptococcaceae* was negatively correlated with HIX and positively correlated with MeHg production in unvegetated microcosms (Pearson's r (n = 6), HIX: r = -0.82, MeHg: r = 0.67). *Peptococcaceae* abundance in vegetated microcosms was not strongly correlated with HIX (r = -0.49) or MeHg production (r = -0.04).

Finally, despite low statistical power (n = 3), we observed marginally significant trends ($P < 0.10$) between key metabolic pathways and HIX (Table 3). While we note that the sample size for this analysis was low, it is remarkable to observe any trends under this limitation and we provide results as an encouraging avenue for future research. In particular, COGs classified as: Glycosyltransferase, Glycosyltransferases involved in cell wall biogenesis, Glycosyltransferases - probably involved in cell wall biogenesis, and Beta-galactosidase/beta-glucuronidase; and Pfams classified as: Glycosyl transferase family 2, Radical SAM superfamily, and SusD family displayed significant correlations with HIX at the $P < 0.10$ level. Only Pfam PF00593, TonB dependent receptor, correlated with MeHg production ($P < 0.001$, r = -1.00, Table 2).

Discussion.

We show the importance of vegetation patterns and DOM availability in mercury cycling within Lake Superior's St. Louis River Estuary, an integral environment to human society and industries of the region. Our work demonstrates not only the far higher levels of mercury cycling in natural vegetated over unvegetated sediments, but also the susceptibility of oligotrophic,

unvegetated sediments to increases in mercury methylation and changes in microbiome with the addition of DOM. We also suggest a possible involvement of metabolisms that ferment recalcitrant organic matter in mercury methylation, particularly within oligotrophic unvegetated environments. Our results provide a basis for further investigation into the role of newly discovered microorganisms in regulating the production of MeHg in the Great Lakes region and further a body of work aimed at understanding and mitigating human exposure to MeHg.

Mercury methylation across environments.

Our work indicated a strongly different capacity of vegetated vs. unvegetated wetland sediments to cycle mercury. Without leachate addition, MeHg production in vegetated sediments was two orders of magnitude higher than in unvegetated sediments (Figure 1). As such, vegetated sediments may be considered potentially important locations for mercury methylation when mercury is present in the environment. Such a dynamic may be due to either higher overall activity of microorganisms or the unique microbiomes contained within these sediments. Within the high-C vegetated environment, leachate did not influence the sediment microbiome or net MeHg production to the same extent as within the more oligotrophic unvegetated environment (Figure 1, Figure S1). Given high ratios of C:N, high OC content, and low NO_3^- concentrations in our vegetated sediment (Table 1), N-limitation may have mitigated net MeHg production in vegetated environments relative to the unvegetated environment (Taylor and Townsend, 2010), which had substantially lower concentrations of all measured C and nutrient concentrations. Both ambient MeHg levels and net MeHg production were dramatically higher in the vegetated environment, supporting other findings that plant-microbe interactions facilitate MeHg production (Gentès et al., 2017; Roy et al., 2009; Windham-Myers et al., 2014; Windham -

Myers et al., 2009). Indeed, the vegetated environment displayed higher ambient DNA concentration and enzyme activities underlying a higher *in situ* rate of biological activity.

By contrast, the unvegetated environment experienced a dramatic increase in MeHg (Figure 1) in response to leachate that correlated with changes in the sediment microbiome (Figure 2 and 3, Figure S1). Carbon limitation has been widely demonstrated as a constraint on microbial activity (Bradley et al., 1992; Brooks et al., 2005; Wett and Rauch, 2003); thus, leachate may bolster MeHg production in C-limited ecosystems via impacts on microbial activity. In our system, net MeHg production in the unvegetated environment was possibly also constrained by low *in situ* rates of microbial activity and by low N concentration, and net MeHg production in response to leachate stimulus never increased to vegetated levels. Importantly, leachate enhanced the relative abundance of specific putative methylators, indicating that mercury methylation rates may be dually influenced by the sediment microbiome and by organic matter (Aiken et al., 2011; Hsu-Kim et al., 2013).

Microbiome response to leachate addition.

Microbiome responses to leachate in both sediment types are consistent with recent work demonstrating the fermentation of organic material (OM) by *Clostridia* despite the presence of OM-oxidizing *Deltaproteobacteria* (Reimers et al., 2013) and suggest a possible role for methylating members of *Clostridia* in MeHg production.. Within both environments, leachate altered the sediment microbiome, driven largely by increases in *Clostridia* and decreases in *Deltaproteobacteria*. Unvegetated microcosms displayed greater changes in these clades, supporting a greater role for environmental filtering by DOM within oligotrophic environments (Barberán et al., 2012; Stegen et al., 2012). *Clostridia* are obligate anaerobes with the ability to

produce labile carbon compounds via fermentation of recalcitrant organic matter (Reimers et al., 2013; Ueno et al., 2016). Recent work has shown organic carbon degradation via *Clostridial* fermentation to operate at comparable rates to more energetically favorable carbon processing pathways (Reimers et al., 2013). Organic acids (*e.g.*, lactate and acetate) produced through these pathways can also be utilized as a carbon source by sulfate- and iron- reducing *Deltaproteobacteria* (Guerrero-Barajas et al., 2011; Reimers et al., 2013; Zhao et al., 2008). Thus, enhanced DOM breakdown by *Clostridia* may support other biogeochemical cycles that rely on organic carbon as an energy source.

In unvegetated sediments, metagenomic analyses indicated an increase in carbon, and secondarily, iron metabolisms consistent with clades known to methylate mercury, although no methylating pathways could be identified in this work (Gilmour et al., 2013; Hamelin et al., 2011; Kerin et al., 2006; Podar et al., 2015). Carbon metabolisms were the primary KEGG category increasing in abundance within metagenomes (Figure 3A), and several COG pathways and Pfams indicated a possible metabolic shift favoring glycosyltransferases that convert starches, sugars, and nitroaromatics into a wide range of compounds (Bowles et al., 2005; Ramli et al., 2015) (Figure 3B and C). Further, metagenomic increases in Beta-galactosidase/beta-glucoronidase (lactose to galactose/glucose)(Martini et al., 1987), sugar phosphate isomerase/epimerases (sugar metabolism)(Yeom et al., 2013), and lactoylglutathione lyase (detoxification for methyglyoxal fermentation byproduct)(Inoue and Kimura, 1995) and the SusD family (glycan binding)(Martens et al., 2009) provide additional evidence for increases in fermentation processes in response to leachate. Increases in TonB dependent receptors (Moeck and Coulton, 1998), amidohydrolase (Seibert and Raushel, 2005), and NRAMP (Cellier et al., 1995) suggest a secondary importance of iron processing and/or transport of large organic

compounds across cellular membranes. Finally, our results provide a possible genetic mechanism connecting iron, sulfur, carbon, and mercury cycling, as the radical SAM superfamily, which facilitates methyl transfers via the use of a [4Fe-S]+ cluster (Booker and Grove, 2010), increased in concert with net MeHg production. In total, the metabolic potential of the sediment microbiome indicates changes in carbon and iron metabolisms within microcosms experiencing higher net MeHg production in response to leachate, supporting past work that suggests a linkage between mercury methylation and these factors (Gilmour et al., 2013; Hamelin et al., 2011; Hsu-Kim et al., 2013; Kerin et al., 2006; Podar et al., 2015).

Lastly, at high taxonomic resolution in both environments, leachate increased the proportion of methylating organisms classified as *Peptococcaceae* within *Clostridia*, despite drastic differences in sediment chemistry (Figure 2B). Specifically, the two OTUs displaying the greatest change are thought to generate energy via organohalide respiration (*D. restrictus*) and fermentative oxidation of organic matter (*S. glycolicus*, also capable of syntrophy)(Han et al., 2011; Stackebrandt, 2014). The relative abundance of *Peptococcaceae* was positively correlated with MeHg production in the unvegetated environment, and other methylating organisms did not increase in abundance, as would be expected if the activity of these organisms was enhanced by leachate.

Associations between microbiology, DOM processing, and net MeHg production.

The processing of proportionally more labile (microbe-preferred) organic matter would be expected to result in increases in HIX. However, changes in these indices within the unvegetated environment suggest substantial recalcitrant organic matter degradation vs. the metabolism of labile substrates (but not the vegetated environment which followed the

expectation of increase HIX). We observed no change in HIX through time in unvegetated microcosms (both leachate and no leachate). This result is reflective of a DOM pool that has stable relative proportions of labile and recalcitrant organic material, indicating equal rates of degradation and/or production of both substrate types (Figure 4C and D). Vegetated microcosms, in contrast, experienced increases in HIX through time that indicate a loss of labile substrate from the fluorescent DOM pool (Figure 4C and D). Further, in leachate unvegetated microcosms, which experienced pronounced changes in the sediment microbiome and high MeHg production, HIX was significantly lower than in all other experimental groups (ANOVA, $P < 0.0001$, all Tukey HSD $P < 0.0001$). While most microorganisms preferentially degrade labile C sources, the degradation of recalcitrant organic matter can contribute substantially to aquatic carbon cycling (Mcleod et al., 2011). Unvegetated microcosms receiving leachate also exhibited large increases in microbially-derived DOM (FI) through time, demonstrating a noticeable contribution of microbial activity to the DOM pool (Figure 4A).

The abundance of methylating *Peptococcaceae* in unvegetated microcosms negatively correlated with HIX, denoting an apparent association of these members or co-occuring community members with DOM processing, but the mechanisms behind these shifts remain unclear. Metabolism of recalcitrant organic matter by fermenting organisms may influence mercury methylation via direct and indirect mechanisms. Members of *Clostridia* can generate MeHg themselves, and *Clostridial* degradation of recalcitrant organic matter can also produce bioavailable carbon substrates for sulfate- and iron- reducing organisms that produce MeHg (Reimers et al., 2013).

While further work with larger sample size is needed, changes in metagenomes in responses to leachate denote interesting metabolic pathways that may be involved in recalcitrant

organic matter processing and MeHg production. For example, both COG and Pfam glycosyltransferases were negatively correlated with HIX, suggesting a role for starch, sugar, and nitroaromatic fermentation in response to DOM loading. As well, a negative correlation between HIX, and the radical SAM superfamily provides a possible mechanistic linkage between methyl transfers and recalcitrant organic matter processing. Conversely, Beta-galactosidase/beta-glucuronidase, and the SusD family were positively correlated with HIX, indicating a co-association with labile C processing rather than recalcitrant organic matter. Only one abundant Pfam – a TonB dependent receptor, signaling enzyme that may be involved in iron cycling (Moeck and Coulton, 1998) – and no COGs was correlated with MeHg production. Although our results do not provide a direct linkage between metabolic pathways and mercury methylation, it is notable that no pathways associations involve sulfate-reducing or methanogenic methylators.

Conclusions.

Our work shows clearly distinct mercury cycling dynamics between the vegetated and unvegetated sediments of the St. Louis River Estuary environment. While substantially greater MeHg production is observed in vegetated sediments, unvegetated sediments stand to respond more strongly to DOM additions in driving increases in MeHg production. We also describe changes in DOM pool properties through time using fluorescence indices that can be readily applied in natural system and may be particularly valuable for monitoring efforts in wetlands of the Great Lakes Region. Moreover, we also observed evidence for changes in the microbiome of both high-C and oligotrophic sediment in response to leachate addition. The oligotrophic environment showed greater responses in the sediment microbiome and in mercury methylation to the addition of DOM, an important insight given increasing risks of anthropogenic

eutrophication. Microbiome shifts towards fermentation pathways, increases in chemoorganotrophic *Clostridia*, degradation of recalcitrant organic matter, and increases in MeHg within oligotrophic environments begin to elucidate the microbial ecology of mercury methylation. Importantly, our results provide evidence for organisms not historically considered in MeHg production and suggest future work into the environmental relevance of these organisms in mercury methylation. Taken together, our research provides new insights into microorganisms impacting MeHg production in natural settings in the Great Lakes region and emphasizes the importance of exploring microbial physiology not typically associated with methylating organisms in enhancing mercury toxicity.

Acknowledgements.

This work was supported by EPA STAR and NOAA NERRS fellowships to EBG and a JGI CSP grant to DRN. We also acknowledge support from the US Department of Energy (DOE), Office of Biological and Environmental Research (BER), as part of Subsurface Biogeochemical Research Program's Scientific Focus Area (SFA) at the Pacific Northwest National Laboratory (PNNL). PNNL is operated for DOE by Battelle under contract DE-AC06-76RLO 1830. We thank Alan Townsend, Teresa Bilinski, Deb Repert, Dick Smith, Steve Schmidt, Sharon Collinge, Garrett Rue, Jess Ebert, Alexis Templeton, and the LSNERR staff for valuable support and feedback during this project. We also thank Axios Review Service for valuable feedback on this manuscript.

Conflict of Interest.

The authors declare no conflict of interest.

References.

Aiken, G.R., Hsu-Kim, H., Ryan, J.N., 2011. Influence of dissolved organic matter on the environmental fate of metals, nanoparticles, and colloids. Environmental science & technology 45, 3196-3201.

Bae, H.-S., Dierberg, F.E., Ogram, A., 2014. Syntrophs Dominate Sequences Associated with the Mercury Methylation-Related Gene hgcA in the Water Conservation Areas of the Florida Everglades. Applied and environmental microbiology 80, 6517-6526.

Barberán, A., Bates, S.T., Casamayor, E.O., Fierer, N., 2012. Using network analysis to explore co-occurrence patterns in soil microbial communities. The ISME journal 6, 343-351.

Benoit, J., Gilmour, C., Heyes, A., Mason, R., Miller, C., 2003. Geochemical and biological controls over methylmercury production and degradation in aquatic ecosystems. ACS symposium series 835, 262-297.

Benson, D.A., Cavanaugh, M., Clark, K., Karsch-Mizrachi, I., Lipman, D.J., Ostell, J., Sayers, E.W., 2013. GenBank. Nucleic acids research 41, D36-D42.

Booker, S.J., Grove, T.L., 2010. Mechanistic and functional versatility of radical SAM enzymes. F1000 Biol. Rep 2, 52.

Bowles, D., Isayenkova, J., Lim, E.-K., Poppenberger, B., 2005. Glycosyltransferases: managers of small molecules. Current opinion in plant biology 8, 254-263.

Boyd, E.S., Yu, R.-Q., Barkay, T., Hamilton, T.L., Baxter, B.K., Naftz, D.L., Marvin-DiPasquale, M., 2017. Effect of salinity on mercury methylating benthic microbes and their activities in Great Salt Lake, Utah. Science of The Total Environment 581, 495-506.

Bradley, P., Fernandez Jr, M., Chapelle, F., 1992. Carbon limitation of denitrification rates in an anaerobic groundwater system. Environmental science & technology 26, 2377-2381.

Branfireun, B.A., Roulet, N.T., Kelly, C., Rudd, J.W., 1999. In situ sulphate stimulation of mercury methylation in a boreal peatland: Toward a link between acid rain and methylmercury contamination in remote environments. Global Biogeochemical Cycles 13, 743-750.

Brooks, P.D., McKnight, D., Elder, K., 2005. Carbon limitation of soil respiration under winter snowpacks: potential feedbacks between growing season and winter carbon fluxes. Global Change Biology 11, 231-238.

Caporaso, J.G., Kuczynski, J., Stombaugh, J., Bittinger, K., Bushman, F.D., Costello, E.K., Fierer, N., Pena, A.G., Goodrich, J.K., Gordon, J.I., 2010. QIIME allows analysis of high-throughput community sequencing data. Nature methods 7, 335-336.

Caporaso, J.G., Lauber, C.L., Walters, W.A., Berg-Lyons, D., Huntley, J., Fierer, N., Owens, S.M., Betley, J., Fraser, L., Bauer, M., 2012. Ultra-high-throughput microbial community analysis on the Illumina HiSeq and MiSeq platforms. The ISME journal 6, 1621-1624.

Cellier, M., Prive, G., Belouchi, A., Kwan, T., Rodrigues, V., Chia, W., Gros, P., 1995. Nramp defines a family of membrane proteins. Proceedings of the National Academy of Sciences 92, 10089-10093.

Christensen, G.A., Wymore, A.M., King, A.J., Podar, M., Hurt, R.A., Santillan, E.U., Soren, A., Brandt, C.C., Brown, S.D., Palumbo, A.V., 2016. Development and validation of broad-range qualitative and clade-specific quantitative molecular probes for assessing mercury methylation in the environment. Applied and environmental microbiology 82, 6068-6078.

Compeau, G., Bartha, R., 1984. Methylation and demethylation of mercury under controlled redox, pH and salinity conditions. Applied and Environmental Microbiology 48, 1203-1207.

Compeau, G., Bartha, R., 1985. Sulfate-reducing bacteria: principal methylators of mercury in anoxic estuarine sediment. Applied and environmental microbiology 50, 498-502.

Docherty, K.M., Young, K.C., Maurice, P.A., Bridgham, S.D., 2006. Dissolved organic matter concentration and quality influences upon structure and function of freshwater microbial communities. Microbial Ecology 52, 378-388.

Drexel, R.T., Haitzer, M., Ryan, J.N., Aiken, G.R., Nagy, K.L., 2002. Mercury (II) sorption to two Florida Everglades peats: Evidence for strong and weak binding and competition by dissolved organic matter released from the peat. Environmental science & technology 36, 4058-4064.

Edgar, R.C., 2013. UPARSE: highly accurate OTU sequences from microbial amplicon reads. Nature methods 10, 996-998.

Fellman, J.B., Hood, E., Spencer, R.G., 2010. Fluorescence spectroscopy opens new windows into dissolved organic matter dynamics in freshwater ecosystems: A review. Limnology and Oceanography 55, 2452-2462.

Finn, R.D., 2012. Pfam: the protein families database. Encyclopedia of Genetics, Genomics, Proteomics and Bioinformatics.

Forsström, L., Roiha, T., Rautio, M., 2013. Responses of microbial food web to increased allochthonous DOM in an oligotrophic subarctic lake. Aquatic microbial ecology 68, 171-184.

Gabor, R.S., Baker, A., McKnight, D.M., Miller, M.P., 2014a. Fluorescence Indices and Their Interpretation. Aquatic Organic Matter Fluorescence, 303.

Gabor, R.S., Eilers, K., McKnight, D.M., Fierer, N., Anderson, S.P., 2014b. From the litter layer to the saprolite: Chemical changes in water-soluble soil organic matter and their correlation to microbial community composition. Soil Biology and Biochemistry 68, 166-176.

Gentès, S., Taupiac, J., Colin, Y., André, J.-M., Guyoneaud, R., 2017. Bacterial periphytic communities related to mercury methylation within aquatic plant roots from a temperate freshwater lake (South-Western France). Environmental Science and Pollution Research 24, 19223-19233.

Gilmour, C.C., Podar, M., Bullock, A.L., Graham, A.M., Brown, S.D., Somenahally, A.C., Johs, A., Hurt Jr, R.A., Bailey, K.L., Elias, D.A., 2013. Mercury methylation by novel microorganisms from new environments. Environmental science & technology 47, 11810-11820.

Gionfriddo, C.M., Tate, M.T., Wick, R.R., Schultz, M.B., Zemla, A., Thelen, M.P., Schofield, R., Krabbenhoft, D.P., Holt, K.E., Moreau, J.W., 2016. Microbial mercury methylation in Antarctic sea ice. Nature microbiology 1, 16127.

Graham, A.M., Aiken, G.R., Gilmour, C.C., 2013. Effect of dissolved organic matter source and character on microbial Hg methylation in Hg–S–DOM solutions. Environmental science & technology 47, 5746-5754.

Graham, E.B., Crump, A.R., Resch, C.T., Fansler, S., Arntzen, E., Kennedy, D.W., Fredrickson, J.K., Stegen, J.C., 2016a. Coupling spatiotemporal community assembly processes to changes in microbial metabolism. Frontiers in Microbiology 7.

Graham, E.B., Crump, A.R., Resch, C.T., Fansler, S., Arntzen, E., Kennedy, D.W., Fredrickson, J.K., Stegen, J.C., 2017. Deterministic influences exceed dispersal effects on hydrologically‐connected microbiomes. Environmental Microbiology 19, 1552-1567.

Graham, E.B., Knelman, J.E., Schindlbacher, A., Siciliano, S., Breulmann, M., Yannarell, A., Beman, J.M., Abell, G., Philippot, L., Prosser, J., 2016b. Microbes as engines of ecosystem function: When does community structure enhance predictions of ecosystem processes? Frontiers in microbiology 7.

Guerrero-Barajas, C., Garibay-Orijel, C., Rosas-Rocha, L.E., 2011. Sulfate reduction and trichloroethylene biodegradation by a marine microbial community from hydrothermal vents sediments. International Biodeterioration & Biodegradation 65, 116-123.

Haitzer, M., Aiken, G.R., Ryan, J.N., 2002. Binding of mercury (II) to dissolved organic matter: the role of the mercury-to-DOM concentration ratio. Environmental Science & Technology 36, 3564-3570.

Hamelin, S., Amyot, M., Barkay, T., Wang, Y., Planas, D., 2011. Methanogens: principal methylators of mercury in lake periphyton. Environmental science & technology 45, 7693-7700.

Hamelin, S., Planas, D., Amyot, M., 2015. Mercury methylation and demethylation by periphyton biofilms and their host in a fluvial wetland of the St. Lawrence River (QC, Canada). Science of the Total Environment 512, 464-471.

Han, C., Mwirichia, R., Chertkov, O., Held, B., Lapidus, A., Nolan, M., Lucas, S., Hammon, N., Deshpande, S., Cheng, J.-F., 2011. Complete genome sequence of Syntrophobotulus glycolicus type strain (FlGlyRT). Standards in genomic sciences 4, 371.

Harmon, S., King, J., Gladden, J., Chandler, G.T., Newman, L., 2005. Mercury body burdens in Gambusia holbrooki and Erimyzon sucetta in a wetland mesocosm amended with sulfate. Chemosphere 59, 227-233.

Harris-Hellal, J., Vallaeys, T., Garnier-Zarli, E., Bousserrhine, N., 2009. Effects of mercury on soil microbial communities in tropical soils of French Guyana. Applied Soil Ecology 41, 59-68.

Hintelmann, H., Keppel‐Jones, K., Evans, R.D., 2000. Constants of mercury methylation and demethylation rates in sediments and comparison of tracer and ambient mercury availability. Environmental toxicology and chemistry 19, 2204-2211.

Hsu-Kim, H., Kucharzyk, K.H., Zhang, T., Deshusses, M.A., 2013. Mechanisms regulating mercury bioavailability for methylating microorganisms in the aquatic environment: a critical review. Environmental science & technology 47, 2441-2456.

Inoue, Y., Kimura, A., 1995. Methylglyoxal and regulation of its metabolism in microorganisms. Advances in microbial physiology 37, 177.

Jeremiason, J.D., Engstrom, D.R., Swain, E.B., Nater, E.A., Johnson, B.M., Almendinger, J.E., Monson, B.A., Kolka, R.K., 2006. Sulfate addition increases methylmercury production in an experimental wetland. Environmental science & technology 40, 3800-3806.

Kanehisa, M., Goto, S., 2000. KEGG: kyoto encyclopedia of genes and genomes. Nucleic acids research 28, 27-30.

Kerin, E.J., Gilmour, C., Roden, E., Suzuki, M., Coates, J., Mason, R., 2006. Mercury methylation by dissimilatory iron-reducing bacteria. Applied and environmental microbiology 72, 7919-7921.

King, J.K., Kostka, J.E., Frischer, M.E., Saunders, F.M., 2000. Sulfate-reducing bacteria methylate mercury at variable rates in pure culture and in marine sediments. Applied and Environmental Microbiology 66, 2430-2437.

Knelman, J.E., Legg, T.M., O'Neill, S.P., Washenberger, C.L., González, A., Cleveland, C.C., Nemergut, D.R., 2012. Bacterial community structure and function change in association with colonizer plants during early primary succession in a glacier forefield. Soil Biology and Biochemistry 46, 172-180.

Lambertsson, L., Nilsson, M., 2006. Organic material: the primary control on mercury methylation and ambient methyl mercury concentrations in estuarine sediments. Environmental science & technology 40, 1822-1829.

Liu, Y.-R., Yu, R.-Q., Zheng, Y.-M., He, J.-Z., 2014a. Analysis of the Microbial Community Structure by Monitoring an Hg Methylation Gene (hgcA) in Paddy Soils along an Hg Gradient. Applied and environmental microbiology 80, 2874-2879.

Liu, Y.-R., Zheng, Y.-M., Zhang, L.-M., He, J.-Z., 2014b. Linkage between community diversity of sulfate-reducing microorganisms and methylmercury concentration in paddy soil. Environmental Science and Pollution Research 21, 1339-1348.

Lozupone, C., Lladser, M.E., Knights, D., Stombaugh, J., Knight, R., 2011. UniFrac: an effective distance metric for microbial community comparison. The ISME journal 5, 169.

Lu, X., Liu, Y., Johs, A., Zhao, L., Wang, T., Yang, Z., Lin, H., Elias, D.A., Pierce, E.M., Liang, L., 2016. Anaerobic mercury methylation and demethylation by Geobacter bemidjiensis Bem. Environmental science & technology 50, 4366-4373.

Markowitz, V.M., Chen, I.-M.A., Palaniappan, K., Chu, K., Szeto, E., Grechkin, Y., Ratner, A., Jacob, B., Huang, J., Williams, P., 2012. IMG: the integrated microbial genomes database and comparative analysis system. Nucleic acids research 40, D115-D122.

Martens, E.C., Koropatkin, N.M., Smith, T.J., Gordon, J.I., 2009. Complex glycan catabolism by the human gut microbiota: the Bacteroidetes Sus-like paradigm. Journal of Biological Chemistry 284, 24673-24677.

Martini, M.C., Bollweg, G.L., Levitt, M.D., Savaiano, D.A., 1987. Lactose digestion by yogurt beta-galactosidase: influence of pH and microbial cell integrity. The American journal of clinical nutrition 45, 432-436.

Mcleod, E., Chmura, G.L., Bouillon, S., Salm, R., Björk, M., Duarte, C.M., Lovelock, C.E., Schlesinger, W.H., Silliman, B.R., 2011. A blueprint for blue carbon: toward an improved understanding of the role of vegetated coastal habitats in sequestering CO2. Frontiers in Ecology and the Environment 9, 552-560.

Moeck, G.S., Coulton, J.W., 1998. TonB‐dependent iron acquisition: Mechanisms of siderophore‐mediated active transport. Molecular microbiology 28, 675-681.

Morel, F.M., Kraepiel, A.M., Amyot, M., 1998. The chemical cycle and bioaccumulation of mercury. Annual review of ecology and systematics, 543-566.

Parks, J.M., Johs, A., Podar, M., Bridou, R., Hurt, R.A., Smith, S.D., Tomanicek, S.J., Qian, Y., Brown, S.D., Brandt, C.C., 2013. The genetic basis for bacterial mercury methylation. Science 339, 1332-1335.

Pernthaler, J., 2013. Freshwater microbial communities, The Prokaryotes. Springer, pp. 97-112.

Podar, M., Gilmour, C.C., Brandt, C.C., Soren, A., Brown, S.D., Crable, B.R., Palumbo, A.V., Somenahally, A.C., Elias, D.A., 2015. Global prevalence and distribution of genes and microorganisms involved in mercury methylation. Science advances 1, e1500675.

Ramli, N., Abd-Aziz, S., Hassan, M.A., Alitheen, N., Kamaruddin, K., 2015. Potential cyclodextrin glycosyltransferase producer from locally isolated bacteria. African Journal of Biotechnology 9, 7317-7321.

Rani, A., Rockne, K.J., Drummond, J., Al-Hinai, M., Ranjan, R., 2015. Geochemical influences and mercury methylation of a dental wastewater microbiome. Scientific reports 5.

Ravichandran, M., 2004. Interactions between mercury and dissolved organic matter—a review. Chemosphere 55, 319-331.

Reimers, C.E., Alleau, Y., Bauer, J.E., Delaney, J., Girguis, P.R., Schrader, P.S., Stecher, H.A., 2013. Redox effects on the microbial degradation of refractory organic matter in marine sediments. Geochimica et Cosmochimica Acta 121, 582-598.

Rothenberg, S.E., Anders, M., Ajami, N.J., Petrosino, J.F., Balogh, E., 2016. Water management impacts rice methylmercury and the soil microbiome. Science of The Total Environment 572, 608-617.

Roy, V., Amyot, M., Carignan, R., 2009. Beaver ponds increase methylmercury concentrations in Canadian shield streams along vegetation and pond-age gradients. Environmental science & technology 43, 5605-5611.

Ruggiero, P., Terzano, R., Spagnuolo, M., Cavalca, L., Colombo, M., Andreoni, V., Rao, M., Perucci, P., Monaci, E., 2011. Hg bioavailability and impact on bacterial communities in a long-term polluted soil. Journal of Environmental Monitoring 13, 145-156.

Schwartz, G.E., Redfern, L.K., Ikuma, K., Gunsch, C.K., Ruhl, L.S., Vengosh, A., Hsu-Kim, H., 2016. Impacts of coal ash on methylmercury production and the methylating microbial community in anaerobic sediment slurries. Environmental Science: Processes & Impacts 18, 1427-1439.

Seibert, C.M., Raushel, F.M., 2005. Structural and catalytic diversity within the amidohydrolase superfamily. Biochemistry 44, 6383-6391.

Si, Y., Zou, Y., Liu, X., Si, X., Mao, J., 2015. Mercury methylation coupled to iron reduction by dissimilatory iron-reducing bacteria. Chemosphere 122, 206-212.

Stackebrandt, E., 2014. The Emended Family Peptococcaceae and Description of the Families Desulfitobacteriaceae, Desulfotomaculaceae, and Thermincolaceae, The Prokaryotes. Springer, pp. 285-290.

Stegen, J.C., Fredrickson, J.K., Wilkins, M.J., Konopka, A.E., Nelson, W.C., Arntzen, E.V., Chrisler, W.B., Chu, R.K., Danczak, R.E., Fansler, S.J., 2016. Groundwater–surface water mixing shifts ecological assembly processes and stimulates organic carbon turnover. Nature communications 7.

Stegen, J.C., Lin, X., Konopka, A.E., Fredrickson, J.K., 2012. Stochastic and deterministic assembly processes in subsurface microbial communities. The ISME journal 6, 1653-1664.

Tatusov, R.L., Fedorova, N.D., Jackson, J.D., Jacobs, A.R., Kiryutin, B., Koonin, E.V., Krylov, D.M., Mazumder, R., Mekhedov, S.L., Nikolskaya, A.N., 2003. The COG database: an updated version includes eukaryotes. BMC bioinformatics 4, 1.

Taylor, P.G., Townsend, A.R., 2010. Stoichiometric control of organic carbon–nitrate relationships from soils to the sea. Nature 464, 1178-1181.

Ueno, A., Shimizu, S., Tamamura, S., Okuyama, H., Naganuma, T., Kaneko, K., 2016. Anaerobic decomposition of humic substances by Clostridium from the deep subsurface. Scientific reports 6.

Ullrich, S.M., Tanton, T.W., Abdrashitova, S.A., 2001. Mercury in the aquatic environment: a review of factors affecting methylation. Critical reviews in environmental science and technology 31, 241-293.

Waples, J.S., Nagy, K.L., Aiken, G.R., Ryan, J.N., 2005. Dissolution of cinnabar (HgS) in the presence of natural organic matter. Geochimica et Cosmochimica Acta 69, 1575-1588.

Wett, B., Rauch, W., 2003. The role of inorganic carbon limitation in biological nitrogen removal of extremely ammonia concentrated wastewater. Water Research 37, 1100-1110.

Wetzel, R.G., 1992. Gradient-dominated ecosystems: sources and regulatory functions of dissolved organic matter in freshwater ecosystems, Dissolved organic matter in lacustrine ecosystems. Springer, pp. 181-198.

Windham-Myers, L., Marvin-DiPasquale, M., Stricker, C.A., Agee, J.L., Kieu, L.H., Kakouros, E., 2014. Mercury cycling in agricultural and managed wetlands of California, USA:

Experimental evidence of vegetation-driven changes in sediment biogeochemistry and methylmercury production. Science of the Total Environment 484, 300-307.

Windham‐Myers, L., Marvin‐Dipasquale, M., Krabbenhoft, D.P., Agee, J.L., Cox, M.H., Heredia‐Middleton, P., Coates, C., Kakouros, E., 2009. Experimental removal of wetland emergent vegetation leads to decreased methylmercury production in surface sediment. Journal of Geophysical Research: Biogeosciences (2005–2012) 114.

Yeom, S.-J., Kim, Y.-S., Oh, D.-K., 2013. Development of Novel Sugar Isomerases by Optimization of Active Sites in Phosphosugar Isomerases for Monosaccharides. Applied and environmental microbiology 79, 982-988.

Yu, R.-Q., Reinfelder, J.R., Hines, M.E., Barkay, T., 2013. Mercury methylation by the methanogen Methanospirillum hungatei. Applied and environmental microbiology 79, 6325-6330.

Zhao, Y., Ren, N., Wang, A., 2008. Contributions of fermentative acidogenic bacteria and sulfate-reducing bacteria to lactate degradation and sulfate reduction. Chemosphere 72, 233-242.

Zhou, Z., Zheng, Y., Shen, J., Zhang, L., Liu, Y., He, J., 2012. Responses of activities, abundances and community structures of soil denitrifiers to short-term mercury stress. Journal of Environmental Sciences 24, 369-375.

Figures.

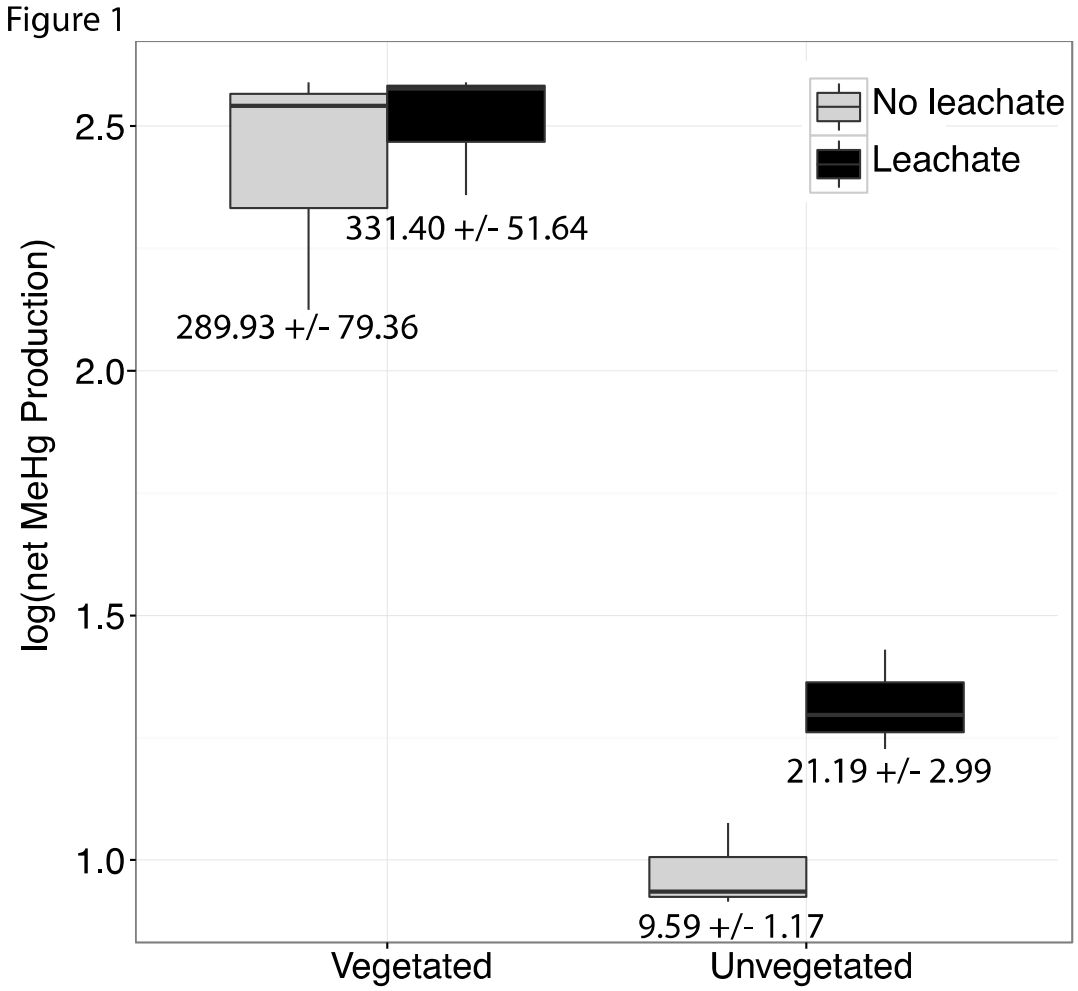

Figure 1. Boxplots are shown for net MeHg production (calculated as concentration at 28 days less the initial concentration), with upper and lower hinges representing the values at the 75th and 25th percentiles and whiskers representing 1.5 times value at the 75th and 25th percentiles, respectively. Leachate increased net MeHg production in unvegetated sediment but did not have a large impact within vegetated sediments. Regardless of leachate addition, vegetated sediment experienced an order of magnitude higher rates of net mercury methylation. All samples were spiked with $HgCl_2$. Mean increase in MeHg production in ng per g dry +/- standard errors are listed below each box.

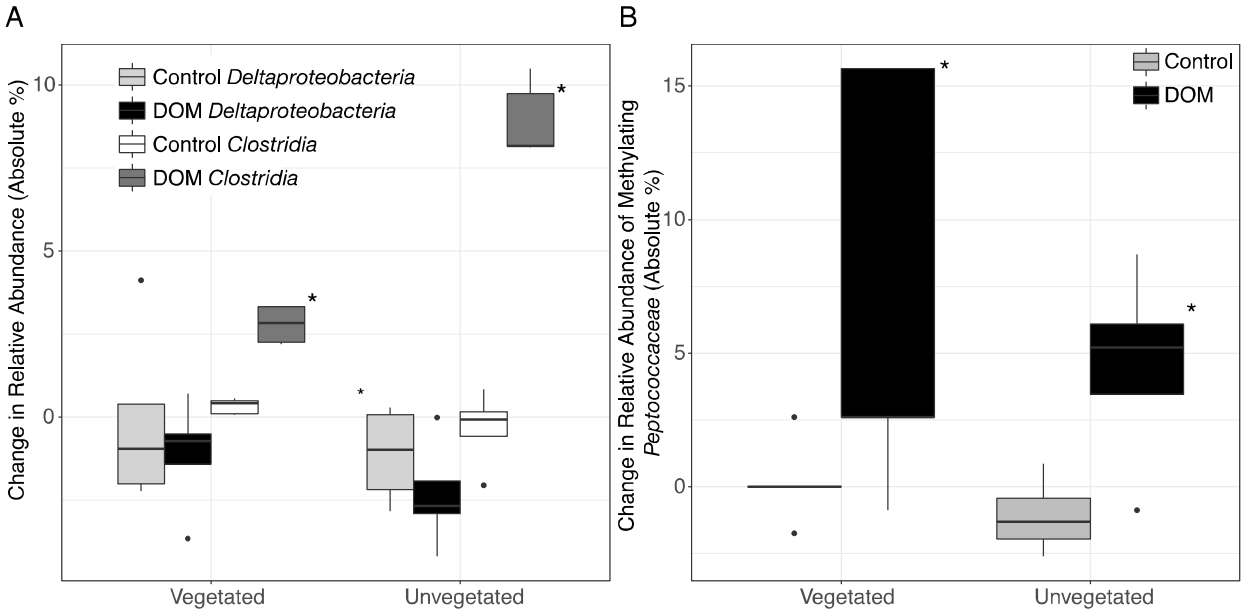

Figure 2. Boxplots are shown for selected changes in taxonomy in response to leachate addition. All samples were spiked with $HgCl_2$. Upper and lower hinges represent values at the 75th and 25th percentiles and whiskers represent 1.5 times values at the 75th and 25th percentiles, respectively. Outliers are plotted as points. Shading for each bar denote taxonomy and leachate vs. no leachate. Significant relationships ($P < 0.05$) are denoted with an asterisk. (A) The addition of leachate decreased the proportion of *Deltaproteobacteria* and increased the proportion of *Clostridia* in both vegetated and unvegetated sediment, with greater effects in unvegetated sediment. (B) Within potential methylators, we observed changes within the family *Peptococcaceae* (class *Clostridia*) in response to leachate addition. Abundance data are present in Table S2.

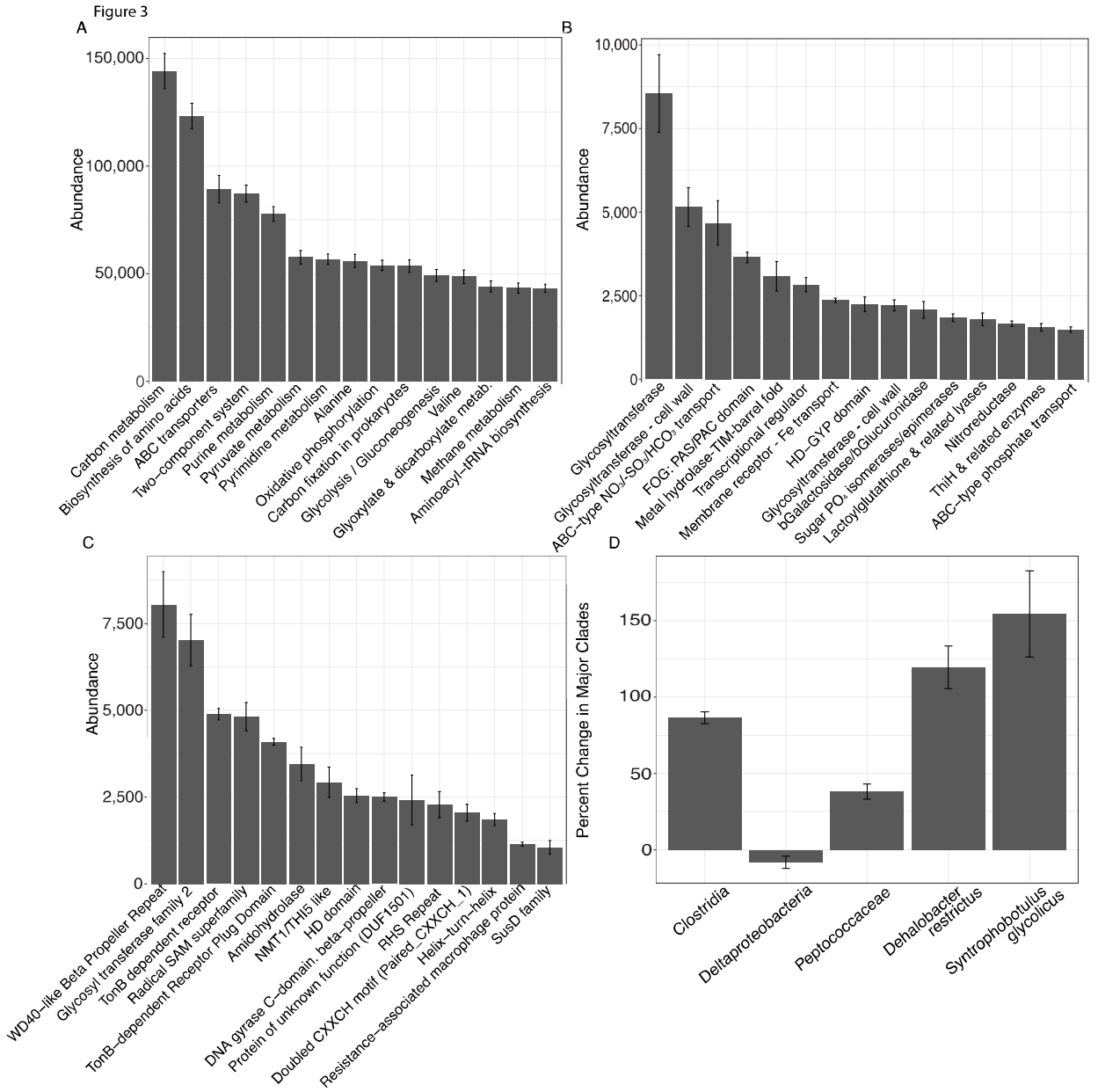

Figure 3. Results from analysis of metagenomic shotgun sequences from unvegetated microcosms are denoted in Figure 3. All samples were spiked with $HgCl_2$. Panels A, B, and C show the abundance of the top 15 KEGG, COG, and Pfam targets that increased at day 28 vs. day 0, respectively. Panel D shows percent change in selected taxonomic groups at day 28 vs. day 0. Error bars denote standard error.

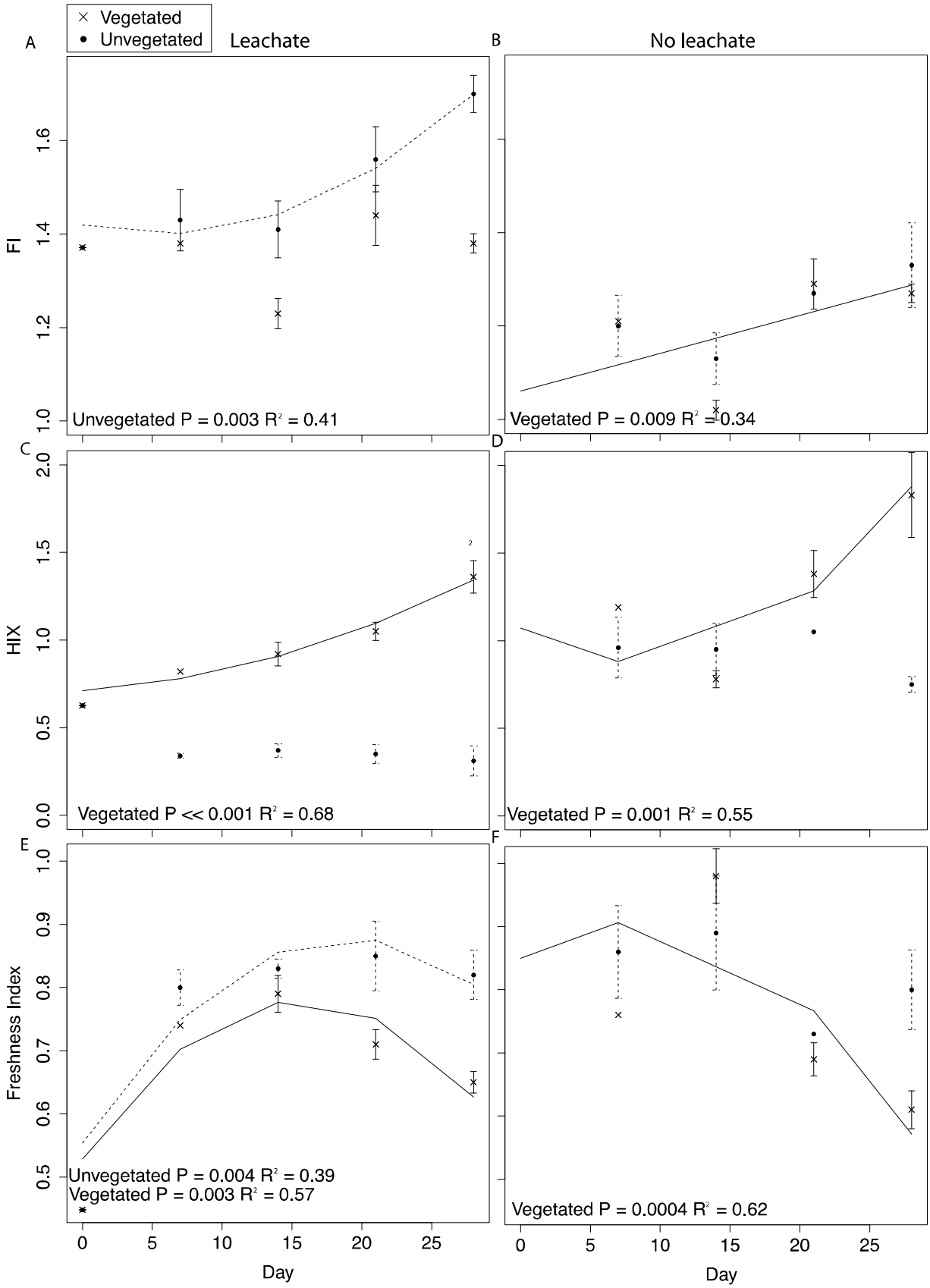
Vegetated
Unvegetated
A
Leachate
B
No leachate
FI
Unvegetated P = 0.003 R² = 0.41
Vegetated P = 0.009 R² = 0.34
C
D
HIX
Vegetated P << 0.001 R² = 0.68
Vegetated P = 0.001 R² = 0.55
E
F
Freshness Index
Unvegetated P = 0.004 R² = 0.39
Vegetated P = 0.003 R² = 0.57
Vegetated P = 0.0004 R² = 0.62
Day
Day

806

Figure 4. DOM fluorescence indices were assessed through time with linear and quadratic regressions in each environment and microcosm type. All samples were spiked with $HgCl_2$. Averages for each environment and microcosm type are plotted at days 0, 7, 14, 21, and 28, with error bars representing the standard error. Plots in the first column are leachate microcosms, while plots in the second column are no leachate microcosms. Unvegetated microcosms are depicted as closed circles with dashed lines showing significant regressions; vegetated microcosms are x's with solid lines showing significant regressions. (A) and (B) denote FI, (C) and (D) denote HIX, and (E) and (F) denote freshness.

Tables.

Table 1. Mean chemical and biological characteristics of vegetated (*n* = 5) and unvegetated (n = 5) environments are presented Table 1. All data are derived from sediments. Asterisks represent significant differences from post hoc *t*-tests, and standard deviations are presented in parentheses. Microbial groups are listed are relative abundance (fraction of all OTUs in community).

	Vegetated Environment	Unvegetated Environment
pH*	5.6 (0.09)	5.8 (0.40)
Water content (g dry/g wet)***	0.54 (0.04)	0.85 (0.04)
NH4 (ug/g wet)***	5.96 (1.28)	1.44 (0.56)
TPOC (ug/g wet)***	90.4 (4.8)	7.2 (4)
TDN (ug/g wet)**	4.8 (1.6)	3.2 (0.8)
percent C***	13.16 (2.20)	1.82 (3.39)
percent N***	0.8 (0.06)	0.1 (0.23)
C:N*	16.43 (1.59)	20.06 (5.36)
DNA concentratin (pg/g wet)***	1.13 (0.20)	0.37 (0.13)
NAG (nmol/h/g)***	308.94 (81.30)	9.05 (9.29)
BG (nmol/h/g)***	371.22 (81.25)	17.71 (19.29)
PHOS (nmol/h/g)***	393.45 (55.06)	20.69 (17.33)
MeHg (ng/g)**	2.67 (2.18)	0.24 (0.12)
THg (ng/g)	306.56 (551.07)	3.16 (3.99)
MeHg:THg	0.02 (0.009)	0.32 (0.45)
Proteobacteria***	0.3 (0.04)	0.43 (0.02)
Chloroflexi***	0.17 (0.01)	0.06 (0.009)
Bacteroidetes	0.11 (0.02)	0.13 (0.03)
Acidobacteria*	0.07 (0.009)	0.08 (0.02)
Nitrospirae***	0.05 (0.009)	0.02 (0.009)
Actinobacteria***	0.03 (0.007)	0.07 (0.01)
Alpha Diversity (PD Whole Tree)**	183.8 (6.64)	193.7 (11.33)
	*P < 0.10	**P < 0.05	***P < 0.01

Table 2. Regression statistics (R^2 values) from analysis of changes in DOM properties through time are listed in Table 2. These values are associated with regressions Presented in Figure 4 and Figure S3. All DOM properties are derived from water overlaying sediments in our incubations. No leachate microcosms were analyzed from across days 7, 14, 21, and 28; and leachate microcosms were analyzed across days 0, 7, 14, 21, and 28 (*n* = 4-5 at each sampling point, no samples were taken in no leachate microcosms at day zero), with characteristics of the applied leachate represented at day 0.

	NPOC (mg/L)	Total Fluoresence	Fluor:NPOC	FI	HIX	Freshness
Vegetated, No leachate (across days 7, 14, 21, 28)	0.39**	0.21*	n.s.	0.22**	0.51***	0.52***
Vegetated, Leachate (across days 0, 7, 14, 21, 28)	0.32***	n.s.	n.s.	n.s.	0.68****	0.57***
Unvegetated, No leachate across days 7, 14, 21, 28)	0.64****	n.s.	0.29**	n.s.	n.s.	n.s.
Unvegetated, Leachate (across days 0, 7, 14, 21, 28)	n.s.	n.s.	n.s.	0.41***	n.s.	0.39***

*$P < 0.10$ **$P < 0.05$ ***$P < 0.01$ ****$P < 0.001$

Table 3. The Pearson product-momentum correlation coefficient was used to assess relationships of selected COG and Pfam targets with HIX and net MeHg production at day 28 (n = 3). Relationships are presented in Table 3.

	HIX	MeHg
COG		
Glycosyltransferase	0.98*	0.79
Glycosyltransferases involved in cell wall biogenesis	0.96*	0.76
ABC-type nitrate/sulfonate/bicarbonate transport systems, periplasmic components	-0.85	0.55
FOG: PAS/PAC domain	-0.88	0.60
Predicted metal-dependent hydrolase of the TIM-barrel fold	0.88	0.60
Transcriptional regulator	0.999**	0.88
Outer membrane receptor proteins, mostly Fe transport	-0.79	0.45
HD-GYP domain	0.99**	0.84
Glycosyltransferases, probably involved in cell wall biogenesis	0.96*	0.74
Beta-galactosidase/beta-glucuronidase	0.98*	-0.80
Sugar phosphate isomerases/epimerases	-0.73	0.36
Lactoylglutathione lyase and related lyases	-0.93	0.67
Nitroreductase	0.996**	0.86
Thiamine biosynthesis enzyme, ThiH and related uncharacterized enzymes	0.98*	0.80
ABC-type phosphate transport system, periplasmic component	-0.66	0.27
Pfam		
WD40-like Beta Propeller Repeat	0.99**	0.85
Glycosyltransferase family 2	0.97*	0.76
TonB dependent receptor	0.90	0.9999***
Radical SAM superfamily	0.95*	0.75
TonB-dependent Receptor Plug Domain	0.51	-0.83
Amidohydrolase	-0.87	0.57
NMT1/THI5 like	-0.87	0.58
HD domain	0.9997**	0.91
DNA gyrase C-terminal domain, beta-propeller	-0.94	0.70
Protein of unknown function (DUF1501)	-0.46	0.04
RHS Repeat	-0.80	0.46
Doubled CXXCH motif (Paired_CXXCH_1)	0.97*	0.78
Helix-turn-helix	-0.90	0.63
Natural resistance-associated macrophage protein	-0.83	0.51
SusD family	0.99*	-0.82

* $P < 0.10$ ** $P < 0.05$